Energy-Efficient Power Allocation for UAV Cognitive Radio Systems

Lokman Sboui[1], Hakim Ghazzai[2], Zouheir Rezki[3], and Mohamed-Slim Alouini[1]

[1]King Abdullah University of Science and Technology (KAUST), Computer, Electrical and Mathematical Science and Engineering Division (CEMSE), Thuwal 23955-6900, Saudi Arabia.
{lokman.sboui, slim.alouini}@kaust.edu.sa

[2]Qatar Mobility Innovations Center (QMIC), Qatar University, Doha, Qatar, hakimg@qmic.com
[3] Department of Electrical and Computer Engineering, University of Idaho, Moscow, ID 83844, USA, zrezki@uidaho.edu

***Abstract*—We study the deployment of unmanned aerial vehicles (UAV) based cognitive system in an area covered by the primary network (PN). An UAV shares the spectrum of the PN and aims to maximize its energy efficiency (EE) by optimizing the transmit power. We focus on the case where the UAV simultaneously communicates with the ground receiver (G), under interference limitation, and with another relaying UAV (A), with a minimal required rate. We analytically develop the power allocation framework that maximizes the EE subject to power budget, interference, and minimal rate constraints. In the numerical results, we show that the minimal rate may cause a transmission outage at low power budget values. We also highlighted the existence of optimal altitudes given the UAV location with respect to the different other terminals.**

***Index Terms*—Cognitive radio systems, energy efficiency, power allocation, unmanned aerial vehicles.**

I. Introduction

Unmanned aerial vehicles (UAVs), or drones, have recently attracted a wide interest for various public, commercial, and industrial applications due to their versatility [1]. Their integration with wireless and mobile networks is expected to bring very high spectral efficiency and offer innovative solutions to solve many communication challenges, particularly for future 5G networks [2]. The rapid and dynamic deployment of UAVs and their reliable line-of-sight (LoS) communication links are the main advantages of UAV-based communications. As a result, this technology is expected provide broa dBand access to remote and inaccessible areas, e.g., areas affected by natural disasters. Also, UAVs will help in facing unexpected congestion situations by providing wireless access for limited time periods such as sports events. Moreover, UAVs can be used for the dispersion, relaying, and collection of data to and from multiple other ground and flying devices, e.g., communicating with ground sensors and other UAVs.

However, UAV-based communication is also facing several challenges that should be addressed to ensure their effective application [3]. One of these challenges is the limited energy availability [4]. In fact, the energy consumption of these battery-powered flying units is usually split into an energy consumed by the communication platform and the energy used for the drone hardware and mobility. Hence, it is important to efficiently manage the available energy for both components in order to save it and hence, extend the UAV operation time before draining its battery. For instance, multiple works in the literature studied the optimal UAV placement that maximizes its performance [5]. Another challenge of deploying UAVs is the spectrum scarcity. Traditionally, UAVs operate at bands that are permanently exploited by other wireless technologies such as the IEEE S-Band, IEEE L-Band and on Industrial, Scientific and Medical (ISM) band [6]. These bands are becoming more and more overcrowded which makes the UAVs suffer from interference caused by the users and vice versa. Hence, cognitive radio (CR) technology for UAV-based communications has been proposed as a potential solution to cope with spectrum congestion in UAV applications [7]–[9].

To address these two major problems in UAV-based communication, we propose to integrate an underlay CR solution with an energy-efficient power allocation scheme in order to ensure effective and long-time operations of UAVs. Given the non-convexity of the EE function, this type of problem is solved via numerical fractional programming algorithms, e.g., [10], [11]. In this paper, we aim to provide explicit expressions of the power solutions in order to decrease the complexity of the power control procedure compared to the numerical methods used in the literature. In this framework, particularly applied for a transmitter drone communicating with ground devices and other flying drones, we formulate an optimization problem aiming at maximizing the energy efficiency of the UAV unit. This is performed while respecting various constraints: (i) a power budget constraint, (ii) a CR underlay constraint forcing the drone to transmit its signal to ground receivers under a certain interference temperature imposed by the license's owner (iii) a QoS constraint ensuring that the data rate between the two flying UAVs to be greater than a certain minimal required rate. An optimal power allocation scheme achieving energy efficient operation of UAVs is developed for unconstrained and multiple-constraints problems. Selected numerical results show that the performance of the proposed scheme versus several system parameters in order to highlight the ability of the proposed approach in increasing the lifetime of the UAV's battery.

The rest of this paper is organized as follows. In Section II, the system model is described. In Section III, the problem formulation is presented. Section IV presents the optimal solutions. Numerical results are presented in Section V. Finally, the paper is concluded in Section VI.

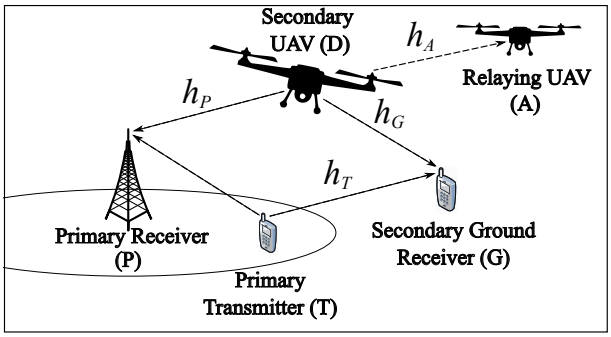

Fig. 1: A cognitive UAV communicating with a ground receiver and a relaying UAV.

II. System Model

We consider a UAV-based system where a drone (D), aims to forward data to two receivers: one ground receiver (G) and a relaying UAV (A), respectively, as shown in Fig. 1. This scenario corresponds, for instance, to a cognitive radio UAV-based communication scenario where a drone collects data from a gateway or ground control center and disseminates it to other ground devices (e.g., sensors) and other UAVs (i.e., a backhaul link) that will themselves broadcast the data to other devices. We assume that each drone, particularly D, is equipped with two antennas with different frequencies. The first antenna communicates with G whereas the second communicates with A. Consequently, we assume that A and G do not see interference from each other. However, the antenna used for the ground communication causes interference to the primary receivers. In fact, the drone D, as a secondary node, opportunistically exploits and shares the primary spectrum for the air to ground transmission. In the same time, a primary transmitter (T) is communicating with the primary receiver (P).

We denote by h_P, h_G, h_T, and h_A the channel gains representing the links between D and P, between D and G, between T and G, and between D and A, respectively. All channel gains are assumed to be independent and constant during the transmission time and full channel state information (CSI) is assumed to be available. The channel gain between the node D and another node Q (Q $\in$ {P, G, A}) including the path loss and fast fading effects is expressed as $h_Q = \frac{\tilde{h}_Q}{\sqrt{PL_Q}}$, where $\tilde{h}_Q$ is the normalized channel vector and PL_Q is the path loss effect between D and Q that are separated by a distance, denoted by d_Q, which corresponds to the Euclidean distance and is expressed as $d_Q = ||\boldsymbol{X}_D - \boldsymbol{X}_Q|| = \left((x_D - x_Q)^2 + (y_D - y_Q)^2 + (z_D - z_Q)^2\right)^{\frac{1}{2}}$ where $\boldsymbol{X}_D$ and $\boldsymbol{X}_Q$ are the geographical coordinates of nodes D and Q, respectively, and $||.||$ is the 2-norm distance. The path loss effect have two forms depending on the availability of the line of sight (LoS) between the nodes. Hence, the free-space path loss effect assuming strict LoS availability, denoted by PL_Q^{LoS} with $Q \in \{P, G, A\}$, is expressed in dB as follows:

$$PL_Q^{\text{LoS}} = 10n \log_{10}\left(\frac{4\pi f d_Q}{C}\right) + L_{\text{LoS}}[\text{dB}], \qquad (1)$$

where n is the path loss exponent, f is the carrier frequency, where C is the speed of light, and where L_{LoS} is the average additional loss due to LoS link that depends on the environment. On the other hand, we denote by PL_Q^{NLoS} the free space path loss corresponding to the non LoS link which is expressed in dB as follows:

$$PL_Q^{\text{NLoS}} = 10n \log_{10}\left(\frac{4\pi f d_Q}{C}\right) + L_{\text{NLoS}}\ [\text{dB}], \qquad (2)$$

where L_{NLoS} is the average additional loss to the free-space propagation loss for the NLoS link.

The fast-fading channel gain, denoted by $\tilde{h}_Q$, corresponds to a Rician fading channel composed of two components: LoS and Rayleigh fading components and is expressed as follows:

$$\tilde{h}_Q = \sqrt{\frac{K}{K+1}}\tilde{h}^{\text{LoS}} + \sqrt{\frac{1}{K+1}}\tilde{h}^{\text{NLoS}}, \qquad (3)$$

where K is the Rician factor, $\tilde{h}^{\text{LoS}}$ is a constant term and corresponds to the LoS component, and $\tilde{h}^{\text{NLoS}}$ corresponds to the NLoS fading component.

Accordingly, three types of channels are considered in this framework depending on the nature of the transmitter and receiver: the air to air (A2A) channel for h_A, the air to ground (A2G) channel for h_P and h_G, and the ground to ground (G2G) channel for h_T. In the sequel, we add the notations (A2A), (A2G), and (G2G) as superscripts for the parameters to distinguish between the channel types.

a) Air to Air Channel: This channel is characterized by a strict availability of line of sight (LoS) between both UAVs. Hence, the A2A path loss $PL_A = PL_A^{\text{LoS}}$. The NLoS fading component is also neglected in the A2A link, i.e., $K^{(\text{A2A})}$ is set close to zero (i.e., $K^{(\text{A2A})} \to 0$).

b) Air to Ground Channel: This case concerns the channels h_P and h_G where the LoS links between the flying drone and ground nodes are assumed to be available with a certain probability denoted by p_Q^{LoS} with Q $\in$ {P, G}. The average A2G free space path loss, denoted by PL_Q, is given as [5]: $PL_Q = p_Q^{\text{LoS}} PL_Q^{\text{LoS}} + (1 - p_Q^{\text{LoS}}) PL_Q^{\text{NLoS}},\ Q \in \{P, G\}$, with $p_Q^{\text{LoS}} = \frac{1}{1+\phi \exp(-\phi[\theta - \psi])}$,where θ is the elevation angle between the nodes D and Q in (degree) which depends on the distance d_Q and ϕ and ψ are constant values that depend on the environment. The fading channel, $\tilde{h}_Q$ where $Q \in \{P, G\}$, is also modeled as a Rician fading channel as (3) with a Rician factor selected such that $\frac{K^{A2G}}{K^{A2G}+1} = p_Q^{\text{LoS}}$.

c) Ground to Ground Channel: This case corresponds to the channel h_T characterized by the strict absence of LoS link between the ground nodes. In this case, the G2G path loss $PL_T = PL_T^{\text{LoS}}$ and the LoS component in (3) is neglected, i.e., $K^{(\text{G2G})}$ is set to ∞ (i.e., $K^{(\text{G2G})} \to +\infty$). We denote by P_G and P_A the transmit power levels of the UAV (D) dedicated to its transmissions over the A2G and A2A links, respectively. We also denote by P_C the circuit power corresponding to both RF chains which is independent of the radiated power [12].

III. Problem Formulation and Unconstrained Optimization

The objective of this study is to determine the power allocation scheme that maximizes the UAV's EE. The scheme involves transmit power levels of the A2G and the A2A links. The power allocation is limited by a power budget constraint

reflecting the battery life of the UAV and by an interference constraint imposed by the primary user on the secondary UAV. A QoS constraint is imposed to the A2A link to ensure a seamless data transfer in the backhaul of the UAV network.

A. UAV EE Expression and Constraints

We consider the global EE of the secondary system [10], [13], [14], defined as the ratio of the spectral efficiency (SE) over the total consumed power defined as follows:

$$EE = \frac{w_G \log_2\left(1+\frac{P_G|h_G|^2}{w_G\sigma^2+Pp|h_T|^2}\right) + w_A \log_2\left(1+\frac{P_A|h_A|^2}{w_A\sigma^2}\right)}{P_C + P_G + P_A}, \tag{4}$$

where w_G and w_A are the bandwidths used for the A2G and A2A communications, respectively, σ^2 is the noise power, and P_P the primary transmitted power. We denote by P_{tot} the available power budget for all the transmissions. Hence, the power budget constraint is given by:

$$P_G + P_A \leq P_{tot}. \tag{5}$$

From another side, the A2G link needs to preserve the QoS of P by respecting the tolerated interference denoted by I_{th}. Hence, the A2G power is constrained as follows:

$$P_G\,|h_P|^2 \leq I_{th}. \tag{6}$$

For the A2A link, the QoS is required to be above a certain level in order to ensure a reliable back haul transmission. Consequently, the rate of the A2A link needs to be higher than a certain rate denoted by R_A. The corresponding QoS constraint is given as follows:

$$w_A \log_2\left(1+\frac{P_A|h_A|^2}{w_A\sigma^2}\right) \geq R_A. \tag{7}$$

B. Unconstrained EE Maximization

Maximizing the unconstrained EE is a preliminary step in finding the power solutions of the constrained problem. We denote by P_G^* and P_A^* the power solutions. We first start by finding P_G^* then P_A^*.

Note that the EE is a continuous, positive and differentiable function with respect to P_G. In addition, we have $\lim_{P_G\to 0} EE = \lim_{P_G\to\infty} EE = 0$. Since the EE is not multimodal with respect to P_G then, it has a global and unique maxima [15] with respect to P_G. This maxima is obtained by finding the root of the first-order derivative of EE. For simplicity, we set $\gamma_G = \frac{|h_G|^2}{w_G\sigma^2+Pp|h_T|^2}$ and $\gamma_A = \frac{|h_A|^2}{w_A\sigma^2}$. The first-order derivative of EE with respect to P_G is given by:

$$\frac{\partial EE}{\partial P_G} = \frac{w_G\gamma_G}{\log(2)(1+P_G\gamma_G)(P_C+P_G+P_A)} - \frac{w_G\log\left(1+P_G\gamma_G\right)+w_A\log\left(1+P_A\gamma_A\right)}{\log(2)\left(P_C+P_G+P_A\right)^2}. \tag{8}$$

We take $w_G = w_A$. Hence, P_G^*, needs to satisfy the following equation:

$$\frac{\gamma_G}{1+P_G^*\gamma_G} = \frac{\log\left(1+P_G^*\gamma_G\right)+\log\left(1+P_A^*\gamma_A\right)}{P_C+P_G^*+P_A^*}. \tag{9}$$

In order to find P_G, we use the lemma in [14] to solve (9) and we obtain:

$$P_G^* = \left[\frac{1}{\gamma_G}\left(\exp\left(1-SR_G+W\left(\frac{\gamma_G SP_G-1}{e^{1-SR_G}}\right)\right)-1\right)\right]^+, \tag{10}$$

where $W(\cdot)$ is the main branch of the W-Lambert function defined over $[-\frac{1}{e},\infty]$ [16] and $[\cdot]^+ = \min\{\cdot,0\}$ and SR_G and SP_G are defined by:

$$SR_G = \log\left(1+P_A^*\gamma_A\right) \text{ and } SP_G = P_C + P_A^*. \tag{11}$$

Since we found a unique root of the first-order derivative of EE with respect to P_G, a similar result is obtained for P_A^* and these roots correspond necessarily to the maxima of the EE. However, we notice that the power levels P_G^*'s are interdependent since SR_G and SP_G include the P_A. We proceed by finding additional equations relating the power levels to avoid the interdependence. By applying equation (9) for P_G and P_A, we obtain the following equalities:

$$\frac{\gamma_G}{1+\gamma_G P_G^*} = \frac{\gamma_A}{1+\gamma_A P_A^*} = \frac{\log(1+\gamma_G P_G^*)+\log(1+\gamma_A P_A^*)}{P_C+P_G^*+P_A^*}. \tag{12}$$

Hence, we have,

$$P_A^* = P_G^* + \frac{1}{\gamma_G} - \frac{1}{\gamma_A}, \tag{13}$$

$$\Rightarrow \log(1+\gamma_A P_A^*) = \log(1+\gamma_G P_G^*) + \log(\frac{\gamma_A}{\gamma_G}). \tag{14}$$

Consequently, by adopting these expressions of the optimality condition in (9), we obtain:

$$SR_G = \frac{1}{2}\log(\frac{\gamma_A}{\gamma_G}) \text{ and } SP_G = \frac{1}{2}(P_C + \frac{1}{\gamma_G} - \frac{1}{\gamma_A}). \tag{15}$$

Hence, by denoting

$$E_{\gamma_G} = \exp\left(1-\frac{1}{2}\log(\frac{\gamma_A}{\gamma_G}) + W\left(\frac{\gamma_G(\frac{1}{2}(P_C+\frac{1}{\gamma_G}-\frac{1}{\gamma_A}))-1}{e^{1-\frac{1}{2}\log(\frac{\gamma_A}{\gamma_G})}}\right)\right) - 1,$$

we obtain

$$P_G^* = P_G^{EE} = \frac{1}{\gamma_G}[E_{\gamma_G}]^+, \tag{16}$$

$$P_A^* = P_A^{EE} = [P_G^* + \frac{1}{\gamma_G} - \frac{1}{\gamma_A}]^+. \tag{17}$$

where P_G^{EE}, P_A^{EE} are the explicit expressions of the energy efficient power allocation (EEPA). Also from (9), we have $EE = \frac{w_G\gamma_G}{\log(2)(1+P_G^*\gamma_G)}$. Hence, the optimal EE is given by

$$EE^* = \frac{w_G\gamma_G}{\log(2)(1+[E_{\gamma_G}]^+)}. \tag{18}$$

IV. EE Maximization with Active Constraints

Determining the expressions of the optimal power solutions of the unconstrained case present a preliminary step to solve the constrained problem. For simplification, we present the constraints (6) and (7) as follows:

$$P_G \leq \widetilde{P}_G \quad \text{where } \widetilde{P}_G = \frac{I_{th}}{|h_P|^2}, \tag{19}$$

$$P_A \geq \widetilde{P}_A \quad \text{where } \widetilde{P}_A = \frac{2^{\frac{R_A}{w_A}} - 1}{\gamma_A}. \tag{20}$$

Hence, the constrained problem is given by:

$$\max_{P_G, P_A \geq 0} \quad EE, \tag{21}$$

$$\text{subject to } (5), (19), (20). \tag{22}$$

Note that P_G^{EE} and P_A^{EE} are the optimal solutions if they satisfy the constraints (5), (19), and (20). However, since $\widetilde{P}_G$ and $\widetilde{P}_A$ depend on the random channels h_P and h_A, respectively, respecting the constraints is not always ensured. Consequently, a comparison between P_G^{EE} and $\widetilde{P}_G$, P_A^{EE} and $\widetilde{P}_A$ should be performed. For instance, if $P_G^{EE} \geq \widetilde{P}_G$ then, the power to be allocated is $\min\{\widetilde{P}_G, P_{tot}\}$. More generally, if there is only a transmission to G, the solution of the problem is

$$P_G^* = \min\{P_G^{EE}, \widetilde{P}_G, P_{tot}\} \text{ and } P_A^* = 0. \tag{23}$$

However, with the power budget constraint, the corresponding cases are multiple depending of the value of P_{tot}. Consequently, we use a graphical representation in Fig. 2 to illustrate power regions and find the corresponding solutions.

A. Case $P_{tot} \geq \widetilde{P}_A$

In this case, the solutions depend on the value of P_{tot} with respect to $\widetilde{P}_{tot} = \widetilde{P}_G + \widetilde{P}_A$ as shown in Fig. 2.

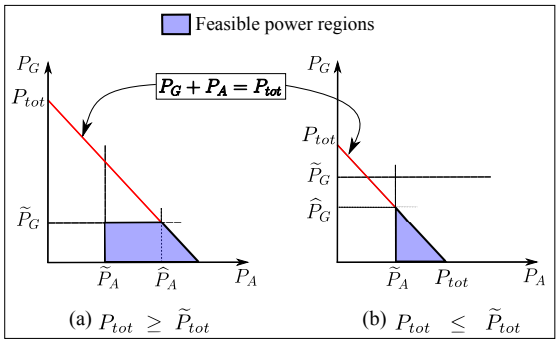

Fig. 2: Regions of feasible power solutions when $P_{tot} \geq \widetilde{P}_A$.

1) $P_{tot} \geq \widetilde{P}_{tot}$: In this case, the feasible region of the power has the shape of a right trapezoid shown in Fig. 2.a. We define $\widehat{P}_A = P_{tot} - \widetilde{P}_G$ and the solution is given depending on the following two subcases:

a) Case $P_A^{EE} \geq \widehat{P}_A$:

- if $P_G^{EE} + P_A^{EE} \leq P_{tot}$ then the EEPA is feasible, i.e.,

$$P_G^* = P_G^{EE} \text{ and } P_A^* = P_A^{EE}. \tag{24}$$

- if $P_G^{EE} + P_G^{EE} \geq P_{tot}$, then the power budget constraint is always active, i.e., $P_G^* + P_A^* = P_{tot}$. Hence, the denominator of the EE is constant, i.e., $EE = \frac{SE}{(P_C + P_{tot})}$ and the corresponding solution is the one that maximizes the SE, i.e., the water-filling power allocation (WPA) [17]. Hence, the solution is given by

$$P_G^* = \min\left\{\widetilde{P}_G, \left[\frac{1}{\log(2)\lambda} - \frac{1}{\gamma_G}\right]^+\right\}, \tag{25}$$

$$P_A^* = \max\left\{\widehat{P}_A, \left[\frac{1}{\log(2)\lambda} - \frac{1}{\gamma_A}\right]^+\right\}, \tag{26}$$

where λ is the Lagrange multiplier associated to P_{tot} computed from (25) such that $P_G^* + P_A^* = P_{tot}$.

b) Case $P_A^{EE} \leq \widehat{P}_A$: In this region, the feasible region is the rectangular part of the trapezoid and the corresponding solution is given by:

$$P_G^* = \min\{P_G^{EE}, \widetilde{P}_G\} \text{ and } P_A^* = \max\{P_A^{EE}, \widetilde{P}_A\}. \tag{27}$$

2) $P_{tot} \leq \widetilde{P}_{tot}$: In this case, the feasible region of the power has the shape of a right triangle. We define $\widehat{P}_G = P_{tot} - \widetilde{P}_A$ and the solution follow two subcases:

a) Case $P_A^{EE} \leq \widetilde{P}_A$:

$$P_G^* = \min\{P_G^{EE}, \widehat{P}_G\} \text{ and } P_A^* = \widetilde{P}_A. \tag{28}$$

b) Case $P_A^{EE} \geq \widetilde{P}_A$:

- if $P_G^{EE} + P_A^{EE} \leq P_{tot}$, the solution is the EEPA as in (24).
- if $P_G^{EE} + P_G^{EE} \geq P_{tot}$, the solution is the WPA as in (25).

B. Case $P_{tot} \leq \widetilde{P}_A$

In this case, the problem does not have any solution since the minimal rate cannot be achieved with the available power budget. Hence, there is no transmission, i.e., $P_G^* = P_A^* = 0$. Alternatively, the UAV may restrict its communication to the ground and transmit with the powers in (23).

V. Numerical Results

In our simulations, we consider that the primary receiver P, the primary transmitter T, the secondary ground receiver G, and the relaying UAV A are located at the following coordinates in meters: $\boldsymbol{X}_P = (0, 0, 1.5)$, $\boldsymbol{X}_T = (50, 0, 0)$, $\boldsymbol{X}_G = (500, 0, 0)$, $\boldsymbol{X}_U = (1000, 1400, 100)$, respectively.

In figures 3, 4 and 5, the coordinates of the transmitting UAV D are $\boldsymbol{X}_D = (500, 50, 100)$. The simulation parameters are given in Table I.

TABLE I: Simulation parameters

Parameter	Value	Parameter	Value
LoS addi. path loss, L_{LoS} (dB)	1	Path loss exponent, n	2
NLoS addi. path loss, L_{NLoS} (dB)	20	LoS prob. parameter, ν_1	9.6
UAV bandwidths, w_G, w_A (kHz)	200	LoS prob. parameter, ν_2	0.29
Primary Trans. Power, P_P (mW)	100	Noise power, σ^2 (dBm/Hz)	-174

In Fig. 3, we plot the EE as function of P_{tot} for different values of P_C. We show that the EE increases with P_{tot} and reaches saturation at P_{tot} higher than $-10, -8$ and -5 dB for P_C equal to 500 mW, 1000 mW and 1500 mW, respectively. Hence, when maximizing the EE the power budget need to be higher than these values to reach the maximum efficiency. In addition, the EE decreases by 45% and by 30% when P_C increases from 500 mW to 1000 mW and from 1000 mW to 1500 mW, respectively. Hence, the RF chain is recommended circuit power even if it requires relatively high P_{tot}, since the EE is almost constant with P_{tot} in high power regime.

In Fig. 4, we plot the EE with different values of R_A. We notice that at some low regions of P_{tot}, the system is in outage. The reason is that the available power budget is not sufficient to transmit with a rate above R_A. Also, the outage region

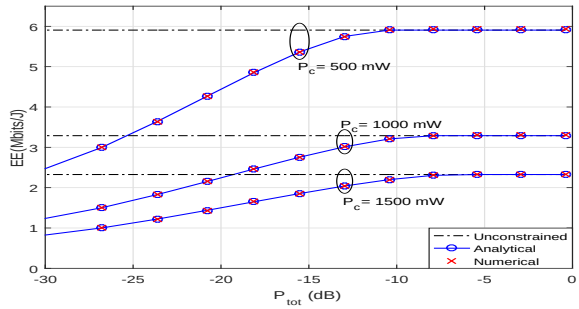

Fig. 3: EE vs. P_{tot} for different P_C with no constraints.

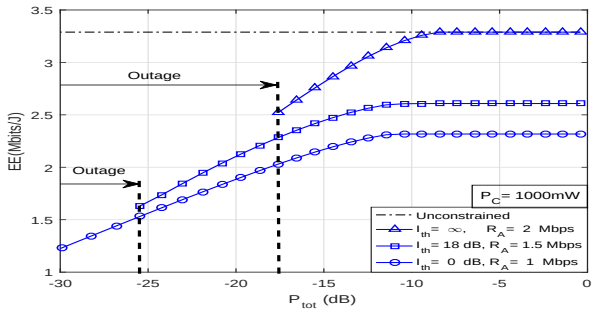

Fig. 4: EE vs. P_{tot} for different values of I_{th} and R_A.

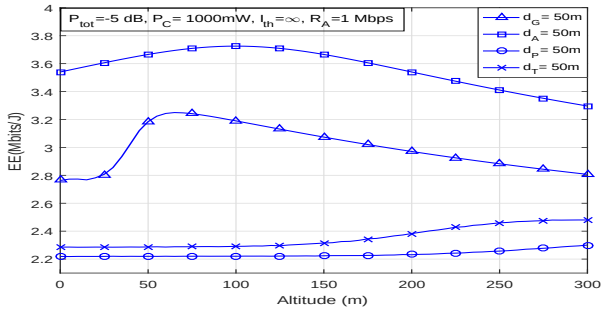

Fig. 5: EE vs. the altitude for the neighborhood of the different terminals.

increases with R_A. For instance, for $R_A = 1.5$ Mbps and 2 Mbps, P_{tot} must be above -26 dB and -17 dB, respectively.

In Fig. 5, we plot the EE as function of D for different locations. The locations are chosen to illustrate the neighborhood of the different terminals. We chose a distance of 50m to reflect the neighborhood of the terminal X, $X \in \{A, G, T, P\}$, i.e., $d_X = 50$m. We show that when the UAV is close to G, there is an optimal altitude, around 65m at which the transmission is the most energy efficient, i.e., more data rate with less power. This observation can be explained by the fact that the channel conditions at low altitude are affected by the absence of direct LoS and hence it increases as the UAV goes higher. Then after the EE peak, the effect of the pathloss affects the performance as the distance between the terminals increases as the UAV flies higher. When the UAV is close to A, located at an altitude of 100m, the EE reaches a maximum value at 100m. This result is expected since the channel is only dictated by the LoS. Finally, when the UAV is close to T or P, the EE slightly increase with the altitude since h_p realizations are smaller causing more relaxed interference constraint.

VI. Conclusion

In this paper, we studied the energy efficiency of a cognitive radio UAV in the presence of primary transmitter and receiver. The UAV performs simultaneous transmission to the ground receiver and to a relaying UAV. We presented an analytical expression of the power that maximizes the EE with no constraints. We then characterized the power control in each power region depending on the channels realizations and the UAV parameters. In the numerical results, we showed that the EE saturates at high power budget values and is highly affected by the circuit power and that the value of the minimal rate may cause transmission outage due to power budget shortage. Finally, we showed that the EE is maximized by being at certain optimal altitude in the neighborhood of another relaying UAV or the ground receiver.

References

[1] "Deliverable D1.5: Updated scenarios, requirements and KPIs for 5G mobile and wireless system with recommendations for future investigations," Tech. Rep., ICT-317669-METIS/D1.5, Sept. 2013.

[2] US Department of Transportation, "Unmanned aircraft system (UAS) service demand 2015-2035: Literature review & projections of future usage," Tech. Rep., v.0.1, DOT-VNTSC-DoD-13-01, Apr. 2015.

[3] Y. Zeng, R. Zhang, and T. J. Lim, "Wireless comm. with unmanned aerial vehicles: opportunities and challenges," *IEEE Comm. Magazine*, vol. 54, no. 5, pp. 36–42, May 2016.

[4] L. Sboui, Z. Rezki, and M.-S. Alouini, "On energy efficient power allocation for Power-Constrained systems," in *Proc. of the IEEE Inter. Symposium on Personal Indoor and Mobile Radio Comm. (PIMRC'14), Washington, DC, USA*, Sep. 2014, pp. 1954–1958.

[5] M. Mozaffari, W. Saad, M. Bennis, and M. Debbah, "Drone small cells in the clouds: Design, deployment and performance analysis," in *in Proc. IEEE Global Telecom. Conf. (GC'15), San Diego, CA, USA*, Dec. 2015.

[6] R. Jain and F. Templin, "Requirements, challenges and analysis of alternatives for wireless datalinks for unmanned aircraft systems," *IEEE J. on Selec. Areas in Comm.*, vol. 30, no. 5, pp. 852–860, June 2012.

[7] L. Sboui, H. Ghazzai, Z. Rezki, and M.-S. Alouini, "On the throughput of cognitive radio MIMO systems assisted with UAV relays," in *Proc. of the Inter. Wireless Comm. and Mobile Computing Conference (IWCMC'17)*, Valencia, Spain, 2017.

[8] ——, "Achievable rates of UAV-relayed cooperative cognitive radio MIMO systems," *IEEE Access*, vol. 5, pp. 5190–5204, 2017.

[9] Y. Saleem, M. H. Rehmani, and S. Zeadally, "Integration of cognitive radio technology with unmanned aerial vehicles: Issues, opportunities, and future research challenges," *Journal of Network and Computer Applications*, vol. 50, pp. 15–31, April 2015.

[10] L. Venturino, A. Zappone, C. Risi, and S. Buzzi, "Energy-efficient scheduling and power allocation in downlink OFDMA networks with base station coordination," *IEEE Trans. on Wireless Comm.*, vol. 14, no. 1, pp. 1–14, Jan. 2015.

[11] D. Ng, E. Lo, and R. Schober, "Energy-efficient resource allocation in OFDMA systems with large numbers of base station antennas," *IEEE Trans. on Wireless Comm.*, vol. 11, no. 9, pp. 3292–3304, Sept. 2012.

[12] L. Sboui, Z. Rezki, and M.-S. Alouini, "Energy-efficient power allocation for underlay cognitive radio systems," *IEEE Trans. on Cognitive Comm. and Networking*, vol. 1, no. 3, pp. 273–283, Sept. 2015.

[13] ——, "Energy-efficient power control for OFDMA cellular networks," in *In Proc. of the IEEE Inter. Symposium on Personal, Indoor, and Mobile Radio Comm. (PIMRC'16), Valencia, Spain*, Sept. 2016, pp. 1–6.

[14] ——, "Energy-efficient power allocation for MIMO-SVD systems," *IEEE Access*, 2017.

[15] G. Miao, N. Himayat, and G. Li, "Energy-efficient link adaptation in frequency-selective channels," *IEEE Trans. on Comm.*, vol. 58, no. 2, pp. 545–554, Feb. 2010.

[16] R. M. Corless, G. H. Gonnet, D. E. Hare, D. J. Jeffrey, and D. E. Knuth, "On the Lambert W function," *Advances in Computational Mathematics*, vol. 5, no. 1, pp. 329–359, 1996.

[17] M. Khoshnevisan and J. Laneman, "Power allocation in multi-antenna wireless systems subject to simultaneous power constraints," *IEEE Trans. on Com.*, vol. 60, no. 12, pp. 3855–3864, Dec. 2012.